Kinetic Model of Product Distribution over Fe Catalyst for Fischer−Tropsch Synthesis†

ARTICLE *in* ENERGY & FUELS · APRIL 2009

Impact Factor: 2.79 · DOI: 10.1021/ef801079u

Energy Fuels **2009,** *23,* 4740–4747 · DOI:10.1021/ef801079u
Published on Web 04/02/2009

energy&fuels
article

Kinetic Model of Product Distribution over Fe Catalyst for Fischer−Tropsch Synthesis†

Rongle Zhang,*,‡ Jie Chang,§ Yuanyuan Xu,‡ Liren Cao,‡ Yongwang Li,‡ and Jinglai Zhou‡

Institute of Coal Chemistry, Chinese Academy of Sciences, Synfuels China, Taoyuan South Road 11, Taiyuan 030001, Shanxi, People's Republic of China, and Institute of Chemical and Engineering Sciences, 1 Pesek Road, Jurong Island, Singapore 627833, Singapore. ‡Chinese Academy of Sciences. §Institute of Chemical and Engineering Sciences.

Received December 15, 2008. Revised Manuscript Received March 9, 2009

A new kinetic model of the Fischer−Tropsch synthesis (FTS) is proposed to describe the non-Anderson−Schulz−Flory (ASF) product distribution. The model is based on the double-polymerization monomers hypothesis, in which the surface C_2* species acts as a chain-growth monomer in the light-product range, while C_1* species acts as a chain-growth monomer in the heavy-product range. The detailed kinetic model in the Langmuir−Hinshelwood−Hougen−Watson type based on the elementary reactions is derived for FTS and the water−gas-shift reaction. Kinetic model candidates are evaluated by minimization of multiresponse objective functions with a genetic algorithm approach. The model of hydrocarbon product distribution is consistent with experimental data ($< C_{45}$). The new model gives a sound interpretation of the experimental data.

1. Introduction

Fischer−Tropsch synthesis (FTS), converting CO and H_2 into hydrocarbons, has drawn renewed attention in recent years.[1] FTS has been recognized as a polymerization reaction. The product yield decreases exponentially with increasing chain growth. The so-called Anderson−Schulz−Flory (ASF) distribution describes the entire product range by a single parameter, α, the probability of the addition of a carbon intermediate to a chain.[2]

However, significant deviations from the ASF distribution are reported in the literature.[3−11] One of the deviations is that the chain-growth factor increased with the carbon number increasing, that is, product distribution frequently characterized as two values of chain-growth factor (2-α). To describe the 2-α phenomenon, several approvals (with and without a physical factor) were made. Konig[3] and Huff[4] suggested a dual active-site mechanism, in which one active site deals with light-hydrocarbon formation and the other deals with the heavier hydrocarbon formation; however, there is no experimental data on the catalyst surface. On the basis of the dissolution and diffusion of olefin in heavier hydrocarbons, Laan[5] and Iglesia[6] indicated that the olefin re-adsorption reaction was responsible for non-ASF distribution, respectively. However, Shi[7,8] and Zhan[9] concluded that diffusion limitations for the olefin products, their subsequent re-incorporation as chain initiators, and the added midcarbon number olefin cannot significantly alter the product distribution in favoring the heavier products. Furthmore, Shi[10] indicated that product accumulation results in the 2-α product distribution ($< C_{20}$), in which the amount of accumulated products was determined accurately in difficulty. Patzlaff[11] and Gaube[12] proposed that supersited two different mechanisms of chain growth result in 2-α product distribution ($< C_{35}$).

Former studies have shown that ethene can act as a chain starter[13−16] and as an intermediate[17,18] that can be inserted into growing chains in the low- and high-carbon ranges. The latter effect of an intermediate in the high-carbon range would probably cause an increased growth probability. Because, in the range of high carbon numbers, the growth probability is not affected by ethene additions, the effect of insertion into a growing chain can be regarded as negligible at least in this range.[11]

If ethene acts as a chain starter, an increased synthesis activity but no change of the growth probability would be expected. However, a decreased formal chain-growth probability in the range of low carbon numbers is observed. It is obvious that chains started with adsorbed ethene grow with a lower probability than chains started in the absence of ethene.[11]

It is valuable that ethene acting as an intermediate inserted into growing chains in the range of low carbon numbers leads to a decreased chain-growth probability. Therefore, all of

† Progress in Coal-Based Energy and Fuel Production.

*To whom correspondence should be addressed. Telephone: +86-351-7560668. Fax: +86-351-7560668. E-mail: zhangrl@sxicc.ac.cn.

(1) Fischer, F.; Tropsch, H. *Brennst. Chem.* **1923**, *4*, 276–285.
(2) van Steen, E.; Schulz, H. *Appl. Catal., A* **1999**, *186*, 309–320.
(3) Konig, L.; Gaube, J. *Chem. Ind. Technol.* **1983**, *55*, 14–18.
(4) Huff, G. A.; Satterfield, C. N. *J. Catal.* **1984**, *85*, 370–379.
(5) van der Laan, G. P.; Beenackers, A. A. C. M. *Ind. Eng. Chem. Res.* **1999**, *38*, 1277–1290.
(6) Iglesia, E.; Reyes, S. C.; Madon, R. J. *J. Catal.* **1991**, *129*, 238–256.
(7) Shi, B.; Jacobs, G.; Sparks, D.; Davis, B. H. *Fuel* **2005**, *84*, 1093–1098.
(8) Shi, B.; Davis, B. H. *Catal. Today* **2005**, *106*, 129–131.
(9) Zhan, X.; Davis, B. H. *Appl. Catal., A* **2002**, *236*, 149–161.
(10) Zhan, X.; Davis, B. H. *Appl. Catal., A* **2004**, *277*, 61–69.
(11) Patzlaff, O.; Liu, Y.; Graffmann, C.; Gaube, J. *Catal. Today* **2002**, *71*, 381–394.
(12) Gaube, J.; Klein, H.-F. *J. Mol. Catal. A: Chem.* **2008**, *283*, 60–68.
(13) Krishna, K. R.; Bell, A. T. *Catal. Lett.* **1992**, *14*, 305–313.
(14) Mims, C. A.; Krajewski, J. J.; Rose, K. D.; Melchior, M. T. *Catal. Lett.* **1990**, *7*, 119–126.
(15) Mims, C. A.; McCandlish, L. E. *J. Phys. Chem.* **1987**, *91*, 929–937.
(16) Turner, M. L.; Marsih, N.; Mann, B. E.; Quyoum, R.; Long, H. C.; Maitlis, P. M. *J. Am. Chem. Soc.* **2002**, *124*, 10456–10472.
(17) Davis, B. H. Mechanism of promotion of iron Fischer−Tropsch catalysts. DOE Final Report 1987; Vol. 3, pp 1−35.
(18) Schulz, H.; Rao, B. R.; Elstner, M. *Erdol Kohle Erdgas Petrochem.* **1970**, *23*, 651–658.

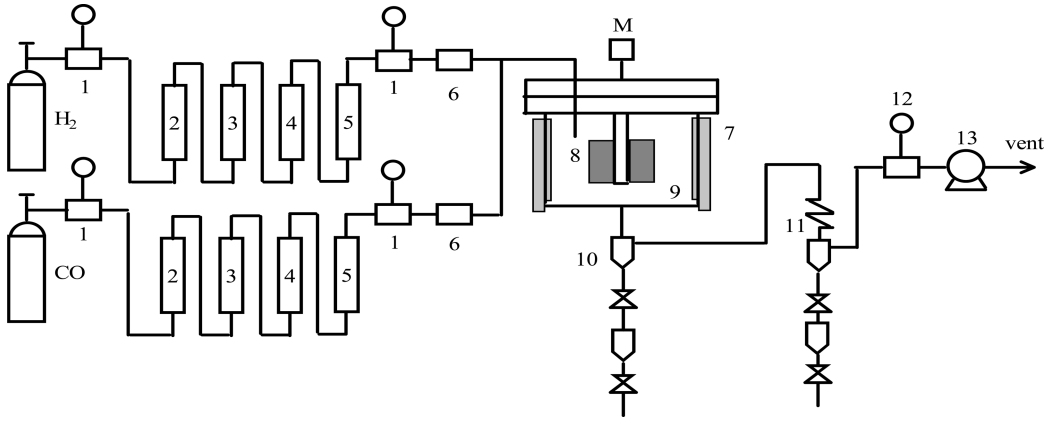

Figure 1. Gradientless reactor experimental setup diagram.

experiments support the theory of superposition of two ASF distributions caused by different chain-growth mechanisms.

The aim of this contribution is to develop a new product distribution model based on ethene re-adsorption and supersited two mechanisms of chain growth, to describe 2-α product distribution.

2. Experimental Section

The experimental setup used in this study is shown in Figure 1. The experiments were carried out in a gas−solid gradientless spinning basket reactor (SBR).[19,20] The catalyst was an industrial copper−potassium-promoted iron catalyst (ICC-IA), prepared by a continuous co-precipitated method[21−23] and formed by spray-dried technology. Before the reaction, the catalyst was reduced *in situ* with syngas ($H_2/CO \sim 2.0$) in the reactor.

The syngas was prepared by blending of pure CO and H_2 (>99.99% purity). The CO and H_2 passed through a series of an oxygen-removal trap, a heated silica gel molecular sieve trap, and an activated charcoal trap to remove tiny amounts of oxygen, water, and other impurities. The flow rates of CO and H_2 were controlled by two Brooks 5850E mass flow controllers. The outlet of the reactor is connected to a hot trap (420 K) and then an ice trap (273 K) at the system pressure. After these product collectors, the pressure was released through a backpressure regulator. The flow rate of the tail gas was monitored by a wet test gas meter.

The products of the synthesis were separated into three portions: the gas phase, liquid phase (from the ice trap), and wax phase (from the hot trap). Both the purified syngas and the tail gas were analyzed on a gas chromatograph. H_2, O_2, N_2, CH_4, and CO were separated on a 13× molecular sieve packed column (1.5 m × 3 mm inner diameter, Ar carrier flow) and detected with a thermal conductivity detector (TCD). C_1-C_5 hydrocarbons in the gas phase were analyzed on a $C_{22}°$ (170−250 μm) packed column (7.2 m × 3.2 mm inner diameter) flame ionization detector (FID), with N_2 as the carrier gas. CO_2 was measured on a silica-gel-packed column (1 m × 3 mm inner diameter, H_2 carrier) with TCD and quantified by an external standard method. The oil product from the cold trap was separated on a 60 m × 0.25 mm (inner diameter) OV-101 capillary column (N_2 carrier, FID), with the temperature programmed from 333 K (maintained for 20 min) to 563 K at the rate of 3 K min^{-1}. The wax product from the hot trap was first dissolved in CS_2 (0.5−1.0 mass %) and then analyzed on a OV-101 capillary column, FID, and N_2 carrier, with the temperature programmed (1 K min^{-1}) from 343 to 563 K. The water phase was separated using a BD-wax (GW, U.S.) capillary column (N_2 carrier, FID). All of the data in steady-state reactions showed promising material balances between 95 and 105%.[24]

In a typical reduction procedure, operation conditions were adjusted to 0.25−0.30 MPa and 1000 h^{-1} at 513 K and then the temperature was raised to 548 K at the rate of 1 K h^{-1} and retained at that temperature for the whole reduction stage. After reduction for 36 h, the temperature was lowered to 513 K and then the operation conditions were adjusted to the desired value for the FTS. For intrinsic kinetic studies, experimental data indicated that the perfect mixing flow was obtained in a sequential batch reactor (SBR) when the stirrer speed was 2000 min^{-1} and gas feed was 500 mL [standard temperature and pressure (STP)]/min; external and internal limitations are insignificant for the stirrer speed = 2000 min^{-1}, $0.147 < d \leq 0.175$ mm.[23,25,26]

For kinetic studies, a stabilization period of more than 100 h was used to ensure that the stable catalytic phases were established.[27,28] Kinetic samples were cumulatively collected during a typical period of 10−16 h. The kinetic experimental conditions were changed as follows: $T = 250-280$ °C, $P = 0.5-1.5$ MPa, H_2/CO feed ratio = 0.71−2.62, and gas hourly space velocity (GHSV) kept stable at 2000 h^{-1}. Experimental results are listed in Table 1.

3. Kinetic Model

3.1. Model Proposed. The FT product distribution is frequently characterized as two values of chain-growth factor (2-α), and the chain-growth factor in the range of a high carbon number is higher than that in the range of a low carbon number. The FT product mainly consisted of α-olefin and paraffin. α-Olefin can be re-adsorped on the catalyst surface and undergo secondary reactions.[7,13] Ethene is the most active α-olefin; its importance in chain growth draws attention. With the (doubly labeled) $^{12}C_2H_4$ cofeeding, Percy[29] indicated that ethene incorporation occurs as a C_2 unit over the Co catalyst. In addition, the ethene inserted

(19) Carberry, J. *J. Ind. Eng. Chem.* **1964**, *11*, 39–45.
(20) Li, Y. W.; Zhang, R. L.; Li, W.; Bai, L.; Xiang, H. W.; Zhou, J. L.; Gao, M. X.; Liu, L.; Chang, J. A kind of reactor evaluating solid catalyst. China Patent ZL 02 2 03353.X, 2002 (in Chinese).
(21) Zhang, Z. X.; Zhou, J. L.; Lin, H. S.; Tang, S. G.; Wang, Q.; Wu, A. P. *Nat. Gas Chem. Ind.* **1991**, *16*, 6–10(in Chinese).
(22) Liu, Z. T.; Li, Y. W.; Zhou, J. L.; Zhang, B. J. *J. Chem. Soc., Faraday Trans.* **1995**, *91*, 3255–3259.
(23) Wang, Y. N.; Ma, W. P.; Lu, Y. J.; Yang, J.; Xu, Y. Y.; Xiang, H. W.; Li, Y. W.; Zhao, Y. L.; Zhang, B. J. *Fuel* **2003**, *82*, 195–213.
(24) Yang, J.; Liu, Y.; Chang, J.; Wang, Y. N.; Bai, L.; Xu, Y. Y.; Xiang, H. W.; Li, Y. W.; Zhong, B. *Ind. Eng. Chem. Res.* **2003**, *42*, 5066–5090.
(25) Lox, E. S.; Froment, G. F. *Ind. Eng. Chem. Res.* **1993**, *32*, 61–82.
(26) Levenspiel, O. *Chemical Reaction Engineering*; Wiley: New York, 1965; Chapter 5.
(27) Jin, Y.; Datye, A. K. *J. Catal.* **2000**, *196*, 8–15.
(28) Burkur, D. B.; Lang, X.; Ding, Y. *Appl. Catal., A* **1999**, *186*, 255–261.
(29) Percy, L. T.; Walter, R. I. *J. Catal.* **1990**, *121*, 228–235.

Table 1. Summary of Kinetic Data (2000 rpm, 2000 h^{-1})

TOS (h)	38	48	90	114	137	148	160	173	195	101	214	246	290	300	312	322
H_2/CO ratio	1.35	1.86	1.86	0.82	1.99	1.35	1.35	0.71	1.35	1.39	0.82	1.86	1.86	0.82	0.82	1.35
P (MPa)	1.0	1.4	0.6	0.6	1.0	1.0	1.0	1.0	0.5	1.5	1.4	1.4	0.6	0.6	1.4	1.0
T (°C)	250	252	252	252	265	265	265	265	265	265	252	277	277	277	277	280
							Conversion (%)									
CO	39.85	63.47	54.13	35.23	76.34	72.78	71.47	56.47	51.56	77.85	62.56	79.67	63.05	46.68	76.09	76.46
$H_2 + CO$	30.17	39.17	32.50	34.10	42.75	48.51	49.49	50.01	37.26	53.70	53.29	50.60	38.18	39.14	65.06	54.02
Q_{WGS}	15.70	12.73	12.78	11.78	16.66	24.45	16.36	13.32	14.32	45.94	16.28	22.63	14.11	12.73	16.81	55.29
K_{eq}	87.10	84.12	84.12	84.12	67.55	67.55	67.55	67.55	67.55	67.55	84.12	55.70	55.70	55.70	55.70	53.16
usage ratio	1.28	1.26	1.39	1.91	1.49	1.76	1.59	1.93	1.43	1.54	1.81	1.22	1.36	1.89	1.79	1.51
selectivity, CO_2 (%)	48.74	49.21	51.69	48.46	43.70	42.73	44.91	50.64	53.04	55.27	46.47	47.49	46.15	49.08	43.37	44.87
							HC Selectivities (wt %)									
C_1	10.48	13.00	12.23	9.41	12.83	12.47	11.58	8.74	10.53	10.36	7.02	16.49	13.96	11.45	8.65	13.59
C_2–C_4	39.24	43.98	39.69	25.24	30.14	26.56	28.89	29.31	25.26	28.93	26.44	35.37	42.40	33.75	26.22	33.58
C_5–C_{11}	15.62	26.89	14.84	14.65	16.58	16.71	14.13	12.04	15.81	16.41	22.87	19.59	16.49	20.46	21.63	21.41
C_{12}+	34.65	16.13	33.24	49.71	40.45	44.26	45.40	49.91	48.40	44.30	43.67	28.54	27.15	34.34	43.50	31.42
							Olefin Selectivity (wt %)									
$C^{=}_2$–$C^{=}_4$	83.39	78.62	79.47	88.29	72.72	77.81	77.69	86.00	82.55	73.55	82.39	66.52	74.83	85.07	77.90	73.80
$C^{=}_5$–$C^{=}_{11}$	76.22	73.99	79.49	70.01	73.46	76.34	76.85	79.92	81.16	81.14	79.60	72.94	79.54	77.82	80.09	79.77
$C^{=}_{12}$–$C^{=}_{20}$	51.18	58.49	49.39	53.37	46.97	46.53	45.33	49.89	59.19	52.75	67.69	39.78	45.16	56.37	58.24	47.73

into growing chains can be divided into a chain starter[13−16] and an intermediate.[17,18] Patzlaff[11] suggested that ethene as a chain starter and as an intermediate[17,18] in the high-carbon range can be neglected because it is inconsistent with the experiment. It might be that ethene acting as an intermediate inserted into growing chains in the range of low carbon numbers leads to a decreased chain-growth probability. Furthermore, the two monomer polymerization hypothesis is proposed. In a lower carbon range, the chain-growth monomer is the C_2* species. In a higher carbon range, the monomer is the C_1* species.

The 2-monomer model can be expressed as follows:

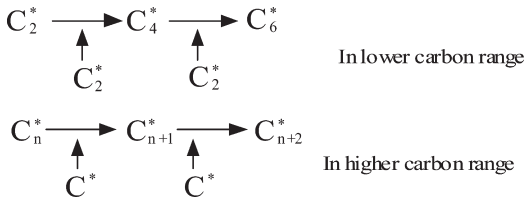

The chain-growth factor is defined

$$\alpha = \frac{R_n}{R_{n-1}} \quad (1)$$

In the lower carbon range, the chain-growth factor is

$$\alpha = \frac{R_n}{R_{n-2}} = \left(\frac{R_n}{R_{n-1}}\right)^2 \quad \text{(lower)} \quad (2)$$

In the higher carbon range, the chain-growth factor is

$$\alpha_2 = \frac{R_n}{R_{n-1}} \quad \text{(higher)} \quad (3)$$

On Fe catalyst, Patzlaff[11] reported that

$$\alpha_1 = 0.49, \quad \alpha_2 = 0.71, \quad \alpha_2^2 - 0.50 \quad (4)$$

$$\text{err} = \frac{\alpha_2^2 - \alpha_1}{\alpha_1} = \frac{0.50 - 0.49}{0.49} \times 100\% = 0.02\% \quad (5)$$

The error is 0.02%. It indicates that different chain-growth monomers lead to different chain-growth factors to some extent; that is, the two monomer polymerization hypothesis is viable.

The experiment illustrated that the cross-point of the product distribution is about C_7.

3.2. Elementary Reaction. In the chain-growth mechanism, the C_1* chain-growth monomer was the first to be considered and then the C_2* chain-growth monomer.

In the kinetic models, the so-called "carbide" mechanism, proposed by Fischer,[1] is chosen as the basis of the elementary reactions.

The key of this mechanism is that the hydrocarbons are built by successive addition of building units with one carbon atom. Five groups of elementary reactions are discussed.

The first group of elementary steps describes the adsorption of carbon monoxide. The adsorption of carbon monoxide is supposed in either the molecule state or the dissociated state, proceeding on a free active site[30−32]

$$CO + s = COs \quad (6)$$

$$COs + s = Cs + Os \quad (7)$$

The second group of elementary reactions deals with the reaction of hydrogen. It is supposed that hydrogen reacted in either the molecular state or the dissociated adsorption.[33,34]

It is assumed that the dissociated adsorption takes place on two adjacent free active sites

$$H_2 + 2s = 2Hs \quad (8)$$

For the reaction of molecular hydrogen, the reaction with a hydrocarbon intermediate via an Eley−Rideal (ER) mechanism is considered[35,36]

$$HCOs + H_2 \leftrightarrow HCs + H_2O \quad (9)$$

$$CH_3COs + H_2 \leftrightarrow CH_3Cs + H_2O \quad (10)$$

The third group of elementary reactions describes the formation of monomers. In the carbide mechanism, there

(30) Li, S.; Meitzner, G. D.; Iglesia, E. *J. Phys. Chem. B* **2001**, *105*, 5743–5749.
(31) Jiang, M.; Koizumi, N.; Yamada, M. *J. Phys. Chem. B* **2000**, *104*, 7636–7643.
(32) Bian, G.; Oonuki, A.; Kobayashi, Y.; Koizumi, N.; Yamada, M. *Appl. Catal., A* **2001**, *219*, 13–24.
(33) Zhang, H. B.; Schrader, G. L. *J. Catal.* **1985**, *95*, 325–332.
(34) Ponec, V.; van Barneveld, W. A. *Ind. Eng. Chem. Prod. Res. Dev.* **1979**, *18*, 268–271.
(35) Wojciechowski, B. W. *Catal. Rev.—Sci. Eng.* **1988**, *30*, 629–643.
(36) Huff, G. A.; Satterfield, C. N. *Ind. Eng. Chem. Process Des. Dev.* **1984**, *23*, 696–703.

are four chain-growth monomers: C, CH, CH_2, and CH_3, respectively.[25,37,38] The propagation of the carbon chain is one monomer by adding one monomer. Here, we consider CH_2 as the monomer to build the kinetic model

$$Cs + Hs = CHs + s \quad (11)$$

$$CHs + Hs = CH_2s + s \quad (12)$$

The fourth group of elementary reactions aims at describing how the carbon chain propagates. There is still a controversy about the mechanism of chain growth in the FTS. The alkyl mechanism proposes that the chain growth takes place by the successive insertion of methylene into the metal−alkyl bond[24]

$$CH_2s + C_nH_{2n+1}s = C_{n+1}H_{2n+3}s + s \quad (13)$$

The alkylidene mechanism proposes that chain growth is facilitated by methylene insertion into the metal−alkylidene bond[39]

$$CH_2s + C_nH_{2n}s = C_{n+1}H_{2n+2}s + s \quad (14)$$

Another mechanism assumes that chain growth is initiated by the insertion of CO into the active sites already containing a hydrocarbon intermediate and then by a sequence of hydrogenation[40,41]

$$C_{n-1}H_{2n-1}s + CO \rightarrow C_{n-1}H_{2n-1}COs \quad (15)$$

$$C_{n-1}H_{2n-1}COs + H_2 \leftrightarrow C_{n-1}H_{2n-1}Cs + H_2O \quad (16)$$

$$C_{n-1}H_{2n-1}Cs + H_2 \leftrightarrow C_{n-1}H_{2n-1}CH_2s \quad (17)$$

The fifth group of elementary reactions deals with the desorption of hydrocarbon products. The desorption of a paraffin may be formed by a single-site reaction with molecular hydrogen

$$C_nH_{2n+1}s + H_2 = C_nH_{2n+2} + Hs \quad (18)$$

or a dual-site reaction with an adsorbed hydrogen atom

$$C_nH_{2n+1}s + Hs = C_nH_{2n+2} + 2s \quad (19)$$

For the desorption of an olefin, a single-site mechanism is assumed in which α-olefins may be formed by a β-hydride elimination reaction

$$C_nH_{2n+1}s = C_nH_{2n} + Hs \quad (20)$$

or a dual-site mechanism

$$C_nH_{2n+1}s + s \rightarrow C_nH_{2n} + Hs + s \quad (21)$$

Ethene in the product is re-adsorption on the catalyst surface and generates the C_2* chain-growth monomer

$$C_2H_4 + s \leftrightarrow C_2H_4s \quad (22)$$

The chain-growth path is as follows:

$$C_{n-1}H_{2n-1}s + C_2H_4s \leftrightarrow C_{n+1}H_{2(n+1)+1}s + s \quad (23)$$

On the basis of above, three sets of elementary reactions are selected, listed in Table 2.

Table 2. Sets of Elementary Reactions for the Reaction Paths Leading to the Hydrocarbon Products

set	number	elementary reaction	
FT I	HC 1	$CO + 2s \leftrightarrow Cs + Os$	
	HC 2	$Cs + Hs \leftrightarrow CHs + s$	
	HC 3	$CHs + Hs \leftrightarrow CH_2s + s$	
	HC 4(n)	$CH_2s + Hs \rightarrow CH_3s + s$	
		$CH_2s + CH_3s \rightarrow CH_3CH_2s + s$	
		$CH_2s + C_nH_{2n+1}s \rightarrow C_nH_{2n+1}CH_2s + s$	($n \geq 7$)
	HC 5(n)	$CH_3s + Hs \rightarrow CH_4 + 2s$	
		$C_nH_{2n+1}s + Hs \rightarrow C_nH_{2n+2} + 2s$	
	HC 6(n)	$C_nH_{2n+1}s + s \rightarrow C_nH_{2n} + Hs + s$	
	HC 7	$H_2 + 2s \leftrightarrow 2Hs$	
	HC 8	$Os + Hs \leftrightarrow HOs + s$	
	HC 9	$HOs + Hs \leftrightarrow H_2O + 2s$	
	HC 10	$C_2H_4 + s \leftrightarrow C_2H_4s$	
	HC 11	$C_{n-1}H_{2n-1}s + C_2H_4s \leftrightarrow C_{n+1}H_{2(n+1)+1}s + s$	($n < 7$)
FT II	HC 1(n)	$Hs + CO \rightarrow HCOs$	
		$CH_3s + CO \rightarrow CH_3COs$	
		$C_{n-1}H_{2n-1}s + CO \rightarrow C_{n-1}H_{2n-1}COs$	($n \geq 7$)
	HC 2(n)	$HCOs + H_2 \leftrightarrow HCs + H_2O$	
		$CH_3COs + H_2 \leftrightarrow CH_3Cs + H_2O$	
		$C_{n-1}H_{2n-1}COs + H_2 \leftrightarrow C_{n-1}H_{2n-1}Cs + H_2O$	
	HC 3(n)	$C_{n-1}H_{2n-1}Cs + H_2 \leftrightarrow C_{n-1}H_{2n-1}CH_2s$	
	HC 4(n)	$C_nH_{2n+1}s + H_2 \rightarrow C_nH_{2n+2} + Hs$	
	HC 5(n)	$C_nH_{2n+1}s \rightarrow C_nH_{2n} + Hs$	
	HC 6	$H_2 + 2s \leftrightarrow 2Hs$	
	HC 7	$C_2H_4 + s \leftrightarrow C_2H_4s$	
	HC 8	$C_{n-1}H_{2n-1}s + C_2H_4s \leftrightarrow C_{n+1}H_{2(n+1)+1}s + s$	($n < 7$)
FT III	HC 1(n)	$Hs + COs \rightarrow HCOs + s$	
		$CH_3s + COs \rightarrow CH_3COs + s$	
		$C_{n-1}H_{2n-1}s + COs \rightarrow C_{n-1}H_{2n-1}COs + s$	($n \geq 7$)
	HC 2(n)	$HCOs + Hs \leftrightarrow HCs + HOs$	
		$CH_3COs + Hs \leftrightarrow CH_3Cs + HOs$	
		$C_{n-1}H_{2n-1}COs + Hs \leftrightarrow C_{n-1}H_{2n-1}Cs + HOs$	
	HC 3(n)	$C_{n-1}H_{2n-1}Cs + Hs \leftrightarrow C_{n-1}H_{2n-1}CHs + s$	
	HC 4(n)	$C_{n-1}H_{2n-1}CHs + Hs \leftrightarrow C_{n-1}H_{2n-1}CH_2s + s$	
	HC 5(n)	$C_{n-1}H_{2n-1}CH_2s + Hs \rightarrow C_nH_{2n+2} + 2s$	
	HC 6(n)	$C_{n-1}H_{2n-1}CH_2s + s \rightarrow C_nH_{2n} + Hs + s$	
	HC 7	$H_2 + 2s \leftrightarrow 2Hs$	
	HC 8	$HOs + Hs \leftrightarrow H_2O + 2s$	
	HC 9	$C_2H_4 + s \leftrightarrow C_2H_4s$	
	HC 10	$C_{n-1}H_{2n-1}s + C_2H_4s \leftrightarrow C_{n+1}H_{2(n+1)+1}s + s$	($n < 7$)
	HC 11	$CO + s \leftrightarrow COs$	

3.3. Kinetic Expression. On the basis of the polymerization mechanism with the C_1* chain-growth monomer, the kinetic expression is deduced. Consider now the case in which there is not a single rate-determining step, for example, the model FT I. Assume that, in all of the reaction paths leading to paraffins, two elementary steps are not in pseudo-equilibrium: HC 4, the propagation of carbon chain, and HC 5, the desorption of paraffin. Similarly, it is assumed that, in all reaction paths leading to olefins, two elementary steps are not in pseudo-equilibrium: again HC 4 and HC 6, the desorption of olefin. In this case

$$R_{C_nH_{2n+2}} = r_5 = k_5[Hs][C_nH_{2n+1}s] \quad (24)$$

$$R_{C_nH_{2n}} = r_6 = k_6[C_nH_{2n+1}s][s] \quad (25)$$

The concentration of the surface intermediates can be expressed as a function of the partial pressure of CO and H_2 by applying the steady-state condition to HC 4−HC 6

$$-\frac{d[C_nH_{2n+1}s]}{dt} = 0 \quad (n = 0, ...) \quad (26)$$

$$r_{n-1,4} - r_{n,4} - r_{n,5} - r_{n,6} = 0 \quad (27)$$

Relation 27 becomes

$$k_4[CH_2s][C_{n-1}H_{2n-1}s] - k_4[CH_2s][C_nH_{2n+1}s] - k_5[Hs][C_nH_{2n+1}s] - k_6[s][C_nH_{2n+1}s] = 0 \quad (28)$$

(37) Liu, Z. P.; Hu, P. *J. Am. Chem. Soc.* **2002**, *124*, 11568–11569.
(38) Itoh, H.; Nagano, S.; Takeda, K.; Kikuchi, E. *Appl. Catal., A* **1993**, *186*, 125–136.
(39) Joyner, R. W. *Catal. Lett.* **1988**, *1*, 307–310.
(40) Vannice, M. A. *Catal. Rev.—Sci. Eng.* **1976**, *14*, 153–191.
(41) Bell, A. T. *Catal. Rev.—Sci. Eng.* **1981**, *23* (1−2), 203–225.

which yields, after rearranging 28

$$\frac{[C_nH_{2n+1}s]}{[C_{n-1}H_{2n-1}s]} = \frac{k_4[CH_2s]}{k_4[CH_2s]+k_5[Hs]+k_6[s]} \quad (29)$$

Considering equilibrium of HC 7 elementary in FT I

$$[Hs] = [K_7P_{H_2}]^{0.5}[s] \quad (30)$$

Similarity of HC 9

$$[HOs] = \frac{P_{H_2O}}{K_9}\frac{1}{K_7^{0.5}P_{H_2}^{0.5}}[s] \quad (31)$$

HC 8

$$[Os] = \frac{1}{K_7K_8K_9}\frac{P_{H_2O}}{P_{H_2}}[s] \quad (32)$$

HC 1

$$[Cs] = K_1K_7K_8K_9\frac{P_{H_2}P_{CO}}{P_{H_2O}}[s] \quad (33)$$

HC 2

$$[CHs] = K_1K_2K_7^{1.5}K_8K_9\frac{P_{H_2}^{1.5}P_{CO}}{P_{H_2O}}[s] \quad (34)$$

HC 3

$$[CH_2s] = K_1K_2K_3K_7^2K_8K_9\frac{P_{H_2}^2P_{CO}}{P_{H_2O}}[s] = M\frac{P_{H_2}^2P_{CO}}{P_{H_2O}}[s] \quad (35)$$

where

$$M = K_1K_2K_3K_7^2K_8K_9 \quad (36)$$

Substitution of 30 and 35 into 29 leads to

$$\frac{[C_nH_{2n+1}s]}{[C_{n-1}H_{2n-1}s]} = \frac{k_4M\frac{P_{H_2}^2P_{CO}}{P_{H_2O}}}{k_4M\frac{P_{H_2}^2P_{CO}}{P_{H_2O}}+k_5K_7^{0.5}P_{H_2}^{0.5}+k_6} \quad (37)$$

Relation 37 is the chain-growth factor

$$\alpha_2 = \frac{k_4M\frac{P_{H_2}^2P_{CO}}{P_{H_2O}}}{k_4M\frac{P_{H_2}^2P_{CO}}{P_{H_2O}}+k_5K_7^{0.5}P_{H_2}^{0.5}+k_6} \quad (38)$$

When $n = 1$, relation 37 becomes

$$[CH_3s] = \frac{k_4M\frac{P_{H_2}^2P_{CO}}{P_{H_2O}}}{k_4M\frac{P_{H_2}^2P_{CO}}{P_{H_2O}}+k_5K_7^{0.5}P_{H_2}^{0.5}+k_6}[Hs] = \frac{k_4M\frac{P_{H_2}^2P_{CO}}{P_{H_2O}}}{k_4M\frac{P_{H_2}^2P_{CO}}{P_{H_2O}}+k_5K_7^{0.5}P_{H_2}^{0.5}+k_6}K_7^{0.5}P_{H_2}^{0.5}[s] = N[s] \quad (39)$$

where

$$N = \alpha K_7^{0.5}P_{H_2}^{0.5} \quad (40)$$

On the catalyst surface, the normalization of the active-site concentration[25]

$$1 = [s]+[Hs]+[Os]+[Cs]+[HOs]+[CHs]+[CH_2s]+[COs]+\sum_{n=1}^{\infty}[C_nH_{2n+1}s] \quad (41)$$

Relation 41 yields, after rearranging

$$[s] = \frac{1}{ss2+N\frac{k_4M\frac{P_{H_2}^2P_{CO}}{P_{H_2O}}+k_5K_7^{0.5}P_{H_2}^{0.5}+k_6}{k_5K_7^{0.5}P_{H_2}^{0.5}+k_6}} \quad (42)$$

where

$$ss1 = 1+K_7^{0.5}P_{H_2}^{0.5}+\frac{1}{K_7K_8K_9}\frac{P_{H_2O}}{P_{H_2}}+K_1K_7K_8K_9\frac{P_{H_2}P_{CO}}{P_{H_2O}}+\frac{1}{K_9K_7^{0.5}}\frac{P_{H_2O}}{P_{H_2}^{0.5}} \quad (43)$$

$$ss2 = ss1+K_1K_2K_7^{1.5}K_8K_9\frac{P_{H_2}^{1.5}P_{CO}}{P_{H_2O}}+K_1K_2K_3K_7^2K_8K_9\frac{P_{H_2}^2P_{CO}}{P_{H_2O}} \quad (44)$$

During the course of the parameter estimation, further simplification in 41 had to be introduced.[25] Formula 41 becomes

$$1 = [s]+[Hs]+\sum_{n=1}^{\infty}[C_nH_{2n+1}s] \quad (45)$$

From 44

$$[s] = \frac{1}{1+K_7^{0.5}P_{H_2}^{0.5}+N\frac{k_4M\frac{P_{H_2}^2P_{CO}}{P_{H_2O}}+k_5K_7^{0.5}P_{H_2}^{0.5}+k_6}{k_5K_7^{0.5}P_{H_2}^{0.5}+k_6}} \quad (46)$$

Substitution of 3, 37, and 46 in 24 and 25 gives the final form of the kinetic expressions

$$R_{C_nH_{2n+2}} = r_5 = k_5K_7^{0.5}P_{H_2}^{0.5}N\alpha^{n-1}[s]^2 \quad (n = 1, 2, ...) \quad (47)$$

$$R_{C_nH_{2n}} = r_6 = k_6N\alpha^{n-1}[s]^2 \quad (n = 2, 3, ...) \quad (48)$$

Formulas 47 and 48 are the kinetic expressions of the polymerization mechanism with the C_1*s chain-growth monomer. As for that with the C_2*s chain-growth monomer, the chain-growth factor, formula 38, becomes

$$\alpha_1 = \frac{K_{10}P_{C_2H_4}}{K_{10}P_{C_2H_4}+k_5K_7^{0.5}P_{H_2}^{0.5}+k_6} \quad (49)$$

The kinetic expressions for the other sets of elementary reactions are derived in a similar way. These formulas are given in Table 3.

For clarity, the hydrocarbon of a carbon number larger than 7 is neglectful in a lower carbon range and so is the hydrocarbon of a carbon number smaller than 7 in a higher carbon range.

3.4. Kinetic Models for the Water−Gas-Shift (WGS) Reaction. On iron catalysts, the WGS reaction mechanism in the literature[42−44] assumed that CO is chemisorbed on the surface of the active phase (Fe_3O_4) as the molecular state, while H_2O was dissociatively adsorbed. The WGS elementary reaction is described in Table 4.

(42) Rethwisch, D. G.; Dumesic, J. A. *J. Catal.* **1986**, *101*, 35–42.
(43) Ovesen, C. V.; Stoltze, P.; Norskov, J. K.; Campbell, C. T. *J. Catal.* **1992**, *134*, 445–468.
(44) Ovesen, C. V.; Clausen, B. S.; Hammershøi, B. S.; Steffensen, G.; Askgaard, T.; Chorkendorff, I.; Nørskov, J. K.; Rasmussen, P. B.; Stoltze, P.; Taylor, P. *J. Catal.* **1996**, *158*, 170–180.

Table 3. Kinetic Expressions Based on Three Sets of Elementary Reactions

model	elementary step not at equilibrium	expression
FT I	HC 4, HC 5, HC 6	$\alpha_1 = \frac{K_{10}P_{C_2H_4}}{K_{10}P_{C_2H_4}+k_5K_7^{0.5}P_{H_2}^{0.5}+k_6}$ $(n<7)$
		$\alpha_2 = \frac{K_M P_{H_2}^2 P_{H_2O}}{K_M P_{H_2}^2 P_{CO}/P_{H_2O}+k_5K_7^{0.5}P_{H_2}^{0.5}+k_6}$ $(n>7)$
		$R_{C_nH_{2n+2}} = r_5 = k_5K_7^{0.5}P_{H_2}^{0.5}N\alpha^{n-1}[s]^2$ $(n=1,2,...)$
		$R_{C_nH_{2n}} = r_6 = k_6N\alpha^{n-1}[s]^2$ $(n=2,3,...)$
		$[s] = \frac{1}{1+K_7^{0.5}P_{H_2}^{0.5}+N\frac{K_M P_{H_2}^2 P_{CO}/P_{H_2O}+k_5K_7^{0.5}P_{H_2}^{0.5}+k_6}{k_5K_7^{0.5}P_{H_2}^{0.5}+k_6}}$
		where $N = \alpha K_7^{0.5}P_{H_2}^{0.5}$, $M = K_1K_2K_3K_7^2K_8K_9$, $K_M = k_4M$
FT II	HC 1, HC 4, HC 5	$\alpha_1 = \frac{K_7P_{C_2H_4}}{K_7P_{C_2H_4}+k_4P_{H_2}+k_5}$ $(n<7)$
		$\alpha_2 = \frac{k_1P_{CO}}{k_1P_{CO}+k_4P_{H_2}+k_5}$ $(n>7)$
		$R_{C_nH_{2n+2}} = k_4K_6^{0.5}P_{H_2}^{1.5}\left(\frac{k_1P_{CO}}{k_1P_{CO}+k_4P_{H_2}}\right)\alpha^{n-1}[s]$ $(n=1,...)$
		$R_{C_nH_{2n}} = k_5K_6^{0.5}P_{H_2}^{0.5}\left(\frac{k_1P_{CO}}{k_1P_{CO}+k_4P_{H_2}}\right)\alpha^{n-1}[s]$ $(n=2,...)$
		$[s] = \frac{1}{1+K_6^{0.5}P_{H_2}^{0.5}+\left(\frac{k_1P_{CO}}{k_1P_{CO}+k_4P_{H_2}}\right)\left(\frac{k_1P_{CO}+k_4P_{H_2}+k_5}{k_1P_{CO}+k_4P_{H_2}}\right)K_6^{0.5}P_{H_2}^{0.5}}$
FT III	HC 1, HC 5, HC 6	$\alpha_1 = \frac{K_9P_{C_2H_4}}{K_9P_{C_2H_4}+k_5K_7^{0.5}P_{H_2}^{0.5}+k_6}$ $(n<7)$
		$\alpha_2 = \frac{k_1K_{11}P_{CO}}{k_1K_{11}P_{CO}+k_5K_7^{0.5}P_{H_2}^{0.5}+k_6}$ $(n>7)$
		$R_{C_nH_{2n+2}} = k_5K_7^{0.5}P_{H_2}^{0.5}M\alpha^{n-1}[s]^2$ $(n=1,...)$
		$R_{C_nH_{2n}} = k_6M\alpha^{n-1}[s]^2$ $(n=2,...)$
		$[s] = \frac{1}{1+\frac{1}{K_7^{0.5}P_{H_2}^{0.5}}+MN}$
		$M = \frac{k_1K_{11}P_{CO}K_7^{0.5}P_{H_2}^{0.5}}{k_1K_{11}P_{CO}+k_5K_7^{0.5}P_{H_2}^{0.5}}$, $N = \frac{k_1K_{11}P_{CO}+k_5K_7^{0.5}P_{H_2}^{0.5}+k_6}{k_5K_7^{0.5}P_{H_2}^{0.5}+k_6}$

Table 4. Elementary Reaction of the WGS Reaction

number	elementary reaction	expressions of rates and equilibrium constants
I	$CO + \sigma = CO - \sigma$	$K_{WGSI} = \frac{[CO-\sigma]}{P_{CO}[\sigma]}$
II	$H_2O + 2\sigma = HO - \sigma + H - \sigma$	$K_{WGSII} = \frac{[HO-\sigma][H-\sigma]}{P_{H_2O}[\sigma]^2}$
III	$CO - \sigma + HO - \sigma = COOH - \sigma + \sigma$	$K_{WGSIII} = \frac{[COOH-\sigma][\sigma]}{[HO-\sigma][H-\sigma]}$
IV	$COOH - \sigma = CO_2 + H - \sigma$	$r_{IV} = k_{WGSIV}[COOH-\sigma] - k_{-WGSIV}[H-\sigma]P_{CO_2}$
V	$2H - \sigma = H_2 + 2\sigma$	$\frac{1}{K_{WGSV}} = \frac{P_{H_2}[\sigma]^2}{[H-\sigma]^2}$
$R_{CO_2} = \frac{k_V(P_{CO}P_{H_2O}/P_{H_2}^{0.5}-P_{CO_2}P_{H_2}^{0.5}/K_P)}{1+K_VP_{CO}P_{H_2O}/P_{H_2}^{0.5}}$, $K_V = K_PK_{WGSIV}K_{WGSV}^{0.5}$, $k_V = K_VK_{WGSIV}$		
$K_P = \frac{5078.0045}{T} - 5.8972089 + 13.958689\times10^{-4}T - 27.592844\times10^{-8}T^2$		

Table 5. Summary of Parameter Estimation Based on Optimal Models

parameter	value	unit	parameter	value	unit
K_M	0.88×10^{-3}	bar^{-2}	$k_{V,0}$	0.13×10^{-2}	mol g^{-1} s^{-1} bar^{-1}
$k_{5,0}$	0.34×10^{-6}	mol g^{-1} s^{-1} bar^{-1}	E_V	113.7	kJ mol^{-1}
E_5	76.2	kJ mol^{-1}	K_V	0.34×10^{-2}	$bar^{-0.5}$
$k_{6,0}$	0.18×10^{-4}	mol g^{-1} s^{-1} bar^{-1}	K_7	0.98	bar^{-1}
E_6	82.8	kJ mol^{-1}	K_{10}	16.5	bar^{-1}

In Table 4, step IV represents the formation of CO_2, by desorption of intermediates, in which the COOH-σ desorption was a rate-determined step (RDS), while other steps (I, II, III, and V) were at equilibrium. The above assumption was supported by the kinetic research on the WGS reaction.[24,25] On the basis of the elementary reaction of WGS, the expression of the CO_2-forming rate is deduced and tabulated in Table 4.

3.5. Model Discrimination and Parameter Estimation. In the kinetics modeling, the *n*-paraffins and 1-olefins, which are dominant in the FT product spectrum, were taken into account, whereas the negligible organic oxygenates were not included.

The gradientless SBR used for the kinetic experiments is simulated by a perfect mixing flow model

$$m_{i,\,out} = m_{i,\,in} + W\sum_{j=1}^{N_R}\alpha_{i,j}R_j \quad (i=1,2,...,N_C;\, j=1,2,...,N_R) \tag{50}$$

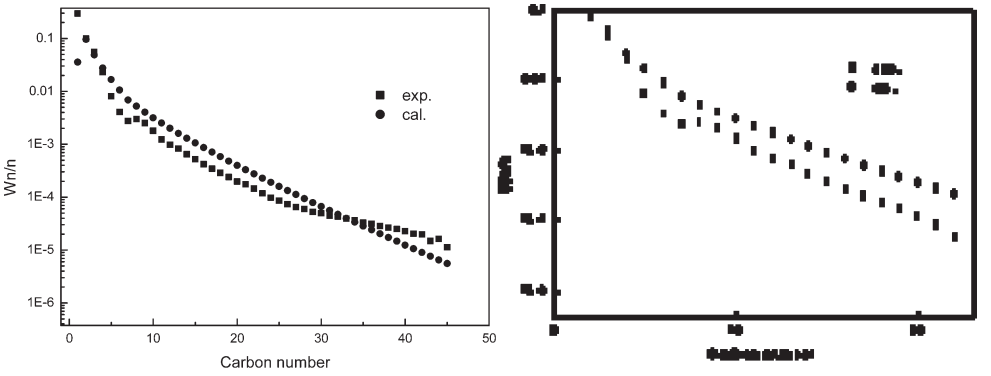

Figure 2. Relationship between the experimental and calculated product distributions of FT I (left, hydrocarbon; right, olefin; conditions, $T = 252$ °C, $P = 1.4$ MPa, H_2/CO feed ratio $= 0.82$).

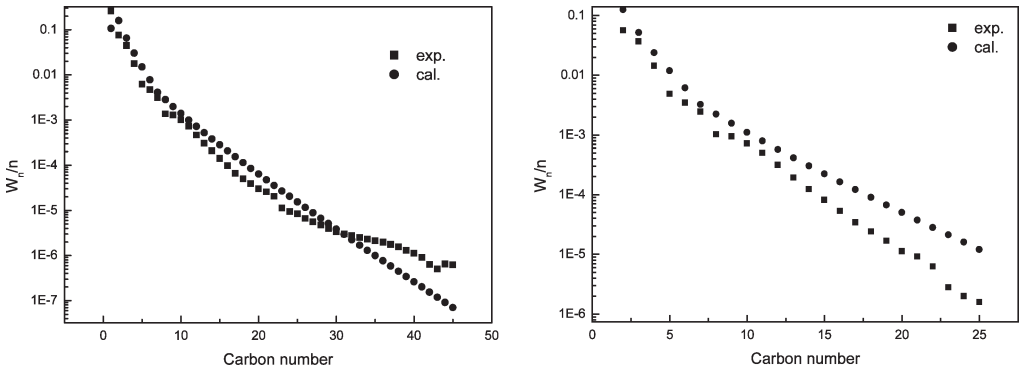

Figure 3. Relationship between the experimental and calculated product distributions of FT I (left, hydrocarbon; right, olefin; conditions, $T = 252$ °C, $P = 1.4$ MPa, H_2/CO feed ratio $= 1.86$).

where W was the weight of the catalyst, $m_{i,\mathrm{out}}$ and $m_{i,\mathrm{in}}$ were the mole flow rate of component i at the outlet and inlet of the reactor, respectively, N_R was the number of reactions involved, N_C was the total number of components, $\alpha_{i,j}$ was the stoichiometric coefficient for the ith component in reaction j,[23−25] and R_j was the rate of reaction j ($R_{C_nH_{2n+2}}$, $R_{C_nH_{2n}}$, and R_{CO_2}).

The dependence of reaction rate parameters on the temperature can be described with the Arrhenius law

$$k_i(T) = k_{i,0} \exp(-E_i/RT) \tag{51}$$

For estimation of the models, 18 objective responses in the regression procedure were the outlet concentrations of 13 paraffins and olefins (such as CH_4, C_2H_4, C_2H_6, C_3H_6, C_3H_8, etc.) selected as the most significant FTS products, accompanied with the concentration of CO_2, conversions of CO and H_2, and overall concentrations of C_5^+ and C_{11}^+ hydrocarbons. The multiresponse objective function[45] was defined as

$$\min(F_{\mathrm{obj}}) = \min\left(\sum_{i=1}^{N_{\mathrm{resp}}}\sum_{j=1}^{N_{\mathrm{exp}}} W_i\left(\frac{m_{ij,\mathrm{exp}} - m_{ij,\mathrm{cal}}}{m_{ij,\mathrm{exp}}}\right)^2\right) \times$$
$$(i = 1, 2, ..., N_{\mathrm{resp}}; j = 1, 2, ..., N_{\mathrm{exp}}) \tag{52}$$

where W_i represented the weight factor of the ith response (represented by the relative importance), N_{resp} was the number of responses in the system, N_{exp} was the kinetic experimental number, $m_{ij,\mathrm{exp}}$ was the experimental value of the ith response for the jth experiment, and $m_{ij,\mathrm{cal}}$ was the calculated value of the ith response for the jth experiment.

The relative residual (RR) between experimental and calculated values of responses would be used to show the deviation between the model and experiment

$$\mathrm{RR}_i = \frac{m_{i,\mathrm{exp}} - m_{i,\mathrm{cal}}}{m_{i,\mathrm{exp}}} \times 100 \tag{53}$$

For estimating parameters, several basic physical criteria were applied: the rate constants and equilibrium constants should be positive, and the activation energies for the paraffin and olefin formations and the WGS reaction should be in the range of values reported by other researchers. The optimization procedure by the genetic algorithm (GA) method[46] had been set to minimize the objective function.

4. Results and Discussion

The discrimination of three rival models is performed by comparing their F_{obj} values. The result shows that the model FT I is the best of the three models. The parameters of model FT I are listed in Table 5. The activation energy of paraffin and olefin formations are 76.2 and 82.8 kJ mol^{-1}, which are in agreement with the literature[31,47,48] (all between 70 and

(45) Himmelblau, D. M.; Jones, C. R.; Bischoff, K. B. *Ind. Eng. Chem. Fundam.* **1967**, *6*, 539–543.

(46) Han, R. F.; Zhang, Y. K.; Wang, Y. N.; Xu, Y. Y.; Li, Y. W. *J. Fuel Chem. Technol.* **2001**, *29*, 371–374(in Chinese).

(47) Huff, G. A.; Satterfield, C. N. *Ind. Eng. Chem. Process Des. Dev.* **1985**, *24*, 986–995.

(48) Dictor, R. A.; Bell, A. T. *J. Catal.* **1986**, *97*, 121–136.

105 kJ mol^{-1}). The adsorption equilibrium constant of ethene is 16.5 bar^{-1}, which is consistent with Zhu.[49]

A comparison between the experimental and calculated product distributions of FT I is presented in Figures 2 and 3. As shown in the figures, the predicted selectivities of olefin are higher than that of the experimental selectivities. However, the selectivities of hydrocarbon predicted are consistent with that of the experimental selectivities and describe the phenomenon that the chain-growth factor increased with the carbon number increasing.

The kinetic model based on the double-polymerization monomer hypothesis primely describes the non-ASF product distribution. It should be noted that the current kinetic model (2-monomer model) has not considered the physical factors (higher olefin effect and accumulated products in the reactor) and only considered the intrinsic kinetic factors (ethene re-adsorption). It is suggested that ethene re-adsorption to enter the hydrocarbon product as the chain-growth monomer plays an important role in non-ASF product distribution.

5. Conclusion

A new product distribution model, which is based on the double-chain growth monomer hypothesis (C^*_1 and C^*_2 species), proves to have a good fit with the deviations from the traditional ASF distribution ($\sim C_{45}$), which were obtained on a spray-dried Fe−Cu−K catalyst in a gas−solid SBR. In the model, the first chain-growth monomer is the C_2^* species before the cross-point and the second chain-growth monomer is the C_1^* species after the cross-point. The detailed kinetic model in the Langmuir−Hinshelwood−Hougen−Watson type was derived for FTS and the WGS reaction, with the assumption that two elementary steps are intrinsically slower than others.

Acknowledgment. The authors gratefully acknowledge the support from the National Natural Sciences Foundation of China (20776146 and 20625620) and the Ministry of Science and Technology of China 973 Project (2007CB216401).

Nomenclature

K_1 = equilibrium constant of elementary reaction 1 for FT I (bar^{-1})
K_2 = equilibrium constant of elementary reaction 2 for FT I
K_3 = equilibrium constant of elementary reaction 3 for FT I
K_7 = equilibrium constant of elementary reaction 7 for FT I (bar^{-1})
K_8 = equilibrium constant of elementary reaction 8 for FT I
K_9 = equilibrium constant of elementary reaction 9 for FT I (bar)
K_{10} = equilibrium constant of elementary reaction 10 for FT I (bar^{-1})
K_M = group of constants of the FT elementary reaction
K_P = equilibrium constant of the WGS reaction
K_V = group of constants of the WGS reaction (bar$^{-0.5}$)
K_{WGSI} = equilibrium constant of the CO adsorption elementary step (bar^{-1})
K_{WGSII} = equilibrium constant of the H_2O adsorption elementary step (bar^{-1})
K_{WGSIII} = equilibrium constant of the surface reaction elementary step
K_{WGSIV} = equilibrium constant of the CO_2 desorption elementary step
K_{WGSV} = equilibrium constant of the H_2 desorption elementary reaction (bar^{-1})
k_4 = rate constant of chain growth (mol g^{-1} s^{-1} bar^{-1})
k_5 = rate constant of the paraffin formation reaction (mol g^{-1} s^{-1} bar^{-1})
k_6 = rate constant of the olefin formation reaction (mol g^{-1} s^{-1} bar^{-1})
E_5 = activation energy for the paraffin formation reaction (kJ mol^{-1})
E_6 = activation energy for the olefin formation reaction (kJ mol^{-1})
E_V = activation energy for the WGS reaction (kJ mol^{-1})
$k_{5,0}$ = pre-exponential factor of the paraffin formation reaction (mol g^{-1} s^{-1} bar^{-1})
$k_{6,0}$ = pre-exponential factor of the paraffin formation reaction (mol g^{-1} s^{-1} bar^{-1})
$k_{V,0}$ = pre-exponential factor of the WGS reaction (mol g^{-1} s^{-1} bar$^{-1.5}$)
m_i = mole flow rate of component i (mol s^{-1})
MARR = mean absolute relative residuals
N = maximum carbon number of the hydrocarbons involved
N_C = total number of components involved
N_R = total number of reactions involved
N_{exp} = total number of experiments
N_{resp} = total number of responses for parameter estimation
P_i = partial pressure of component i (bar)
P_T = total pressure of the reaction system (bar)
R = gas constant (J mol^{-1} K^{-1})
R_j = overall reaction rate of reaction path j (mol g^{-1} s^{-1})
R_i = rate of formation of component i (mol g^{-1} s^{-1})
RR = relative residual between the experimental and calculated values of the response
s = active site for hydrocarbon formation
σ = active site for the WGS reaction
T = temperature of the reaction system (K)
W_i = weight of the ith response
W = weight of the catalyst used (g)

Greek Symbols

α_1 = chain growth factor for the low-carbon range
α_2 = chain growth factor for the high-carbon range
$R_{i,j}$ = stoichiometric coefficient for the ith component in the jth reaction

Superscripts and Subscripts

cal = calculated value
exp = experimental value
i = index indicating reactions
j = index indicating components
n = number of carbon atoms

(49) Zhu, Y. A.; Sui, Zh. J.; Zhao, T. J.; Dai, Y. Ch.; Cheng, Zh. M.; Yuan, W. K. *Carbon* **2005**, *43*, 1694–1699.